Iváñez, I.; Moure, M. M.; García-Castillo, S. K.; Sánchez-Sáez, S. (2015). The oblique impact response of composite sandwich plates. *Composite Structures*, v. 133, pp. 1127-1136.
DOI: 10.1016/j.compstruct.2015.08.035

# The oblique impact response of composite sandwich plates

I. Ivañez *, M.M. Moure, S.K. Garcia-Castillo, S. Sanchez-Saez

*Department of Continuum Mechanics and Structural Analysis, University Carlos III of Madrid, Avda. de la Universidad 30, 28911 Leganés, Madrid, Spain*

*Keywords:*
Angle of obliquity
Sandwich structures
Honeycomb core
Low-velocity impact
Experimental test
Numerical simulation

## Abstract

The following work focus on the experimental study of low velocity oblique impact on composite sandwich plates. Several impact angles and impact energies are selected to study their influence on the maximum contact force, maximum contact time, absorbed energy, maximum displacement of the impactor, and damaged area. Peak load and energy absorption rise with increasing impact energy and impact angle, while the contact time remains almost constant. No major differences in the results are shown for impact angles lower than 15°. In addition, a numerical model is developed to reproduce the experimental results and study the evolution of the main impact results for impact angles difficult to perform experimentally (up to 50°). A good correlation has been found in terms of peak force and contact time, allowing further analysis of the maximum contact force at higher impact angles. Maximum contact force decreases with increasing impact angles, whereas it increases with impact energy until a certain value in which remains almost constant.

## 1. Introduction

Composite sandwich structures are advanced structural composites, with high stiffness to weight ratios, that have been increasingly used in recent years in many lightweight structural applications. Sandwich structures used in high performance aerospace components, are usually based on thin composite face sheets and honeycomb core. Thin composite face sheets show high vulnerability to damage caused by low velocity impact events that can occur during manufacturing, transport, installation, and service operations. In this context, low levels of impact energy can cause none or barely visible impact damage, although may be accompanied by substantial reduction of residual strength (up to 50%) and local stiffness of the composite sandwich structure [1,2].

Many researchers have studied the behaviour of composite sandwich structures under normal impacts [3 11]; however, normal impacts rarely occur in real engineering situations and components are more frequently loaded at some oblique angle. In addition, depending on the angle of incidence of the projectile with respect to the structure, rebounding or ricocheting can occur [12]. A reduced number of studies have focused on the oblique impact response of composites sandwich structures, being most of these works under high velocity impact conditions [13 18].

There is a lack of study on low velocity oblique impact behaviour of composite sandwich structures. Zhou et al. [19] study the effect of angle of obliquity on the perforation resistance of three different sandwich panels based on two crosslinked PVC cores and a PET foam. They develop a numerical analysis of the variation of perforation energy with the angle of obliquity. All three panels exhibited similar response, showing that perforation energy increased with the impact angle. Sheikh et al. [20] study the low velocity oblique impact response of GFRP sandwich foam panels at three impact angles (0°, 10°, and 20°). Similar values of maximum contact force were obtained for the three angles analysed when the impact energy was increased. The damaged area was similar for low impact energies (up to 10 J); however from 10 J, the damaged area was greater at lower impact angles. In addition, they use an analytical model to predict the maximum contact force at varying angles. For impact angle of 0°, the model showed good agreement between predicted and experimental maximum contact force up to 10 J, while above this energy, the model over predicted the maximum contact force. Additionally, the model over predicted the maximum contact force for an angle of 20°, and under predicted the result for an angle of 10°.

The aim of this work is to study the low velocity oblique impact response of composite sandwich plates. Experimental tests on specimens of carbon fibre/epoxy face sheets and Nomex honeycomb core are studied at different impact energies and impactor incidence angles. The influence of the angle of obliquity and the impact energy on the contact force, maximum displacement of the impactor, absorbed energy, and damaged area, are analysed. To study the oblique impact behaviour of impact angles difficult to be conducted experimentally, a finite element model is

* Corresponding author. Tel.: +34 91 624 91 62.
*E-mail address:* idel@ing.uc3m.es (I. Ivañez).

**Table 1**
Properties of the plain weave AS4/8552 given by the manufacturer.

| | | | |
|---|---|---|---|
| $E_1$ (GPa) | 68.5 | $X_T$ (MPa) | 795 |
| $E_2$ (GPa) | 68.5 | $X_C$ (MPa) | 555 |
| $E_3$ (GPa) | 9 | $Y_T$ (MPa) | 795 |
| $\nu_{12}$ | 0.22 | $Y_C$ (MPa) | 555 |
| $\nu_{13}$ | 0.49 | $Z_R$ (MPa) | 74 |
| $\nu_{23}$ | 0.49 | $S_{12}$ (MPa) | 98 |
| $G_{12}$ (GPa) | 3.7 | $S_{13}$ (MPa) | 64 |
| $G_{13}$ (GPa) | 2.5 | $S_{23}$ (MPa) | 64 |
| $G_{23}$ (GPa) | 2.5 | $\rho$ (kg/m$^3$) | 1600 |

implemented. Once validated, the model is used to predict the effect of oblique impact on the maximum contact force.

## 2. Experimental study

### 2.1. Material

Composite sandwich plates tested in this work are based on face sheets of woven carbon fibre reinforced epoxy (AS4/8552), with a thickness of 1.2 mm, and a Nomex honeycomb core HRH 10 1/8 3.0, 10 mm thick. The mechanical properties of the face sheets given by the manufacturer are shown in Table 1.

The combination of carbon fibre reinforced face sheets and Nomex honeycomb core, finds widespread use in the aerospace industry.

### 2.2. Experimental procedure

Low velocity impact tests were performed using an instrumented drop weight tower, CEAST Fractovis 6785. The impactor had a hemispherical tip of 20 mm diameter, and a total mass of 3.620 kg. Specimens had a size of 120 mm × 120 mm, and 12.4 mm thickness.

In order to evaluate the influence of obliquity in the impact behaviour of the sandwich plates, tests were performed using four impact angles (0°, 5°, 10°, and 15°). The impact angle is referred to the angle between the axis of the impactor and the normal to the plate. For each angle of obliquity, tests at several theoretical impact energy levels were performed (3 J, 5 J, 7 J and 10 J). A total of sixteen specimens were tested.

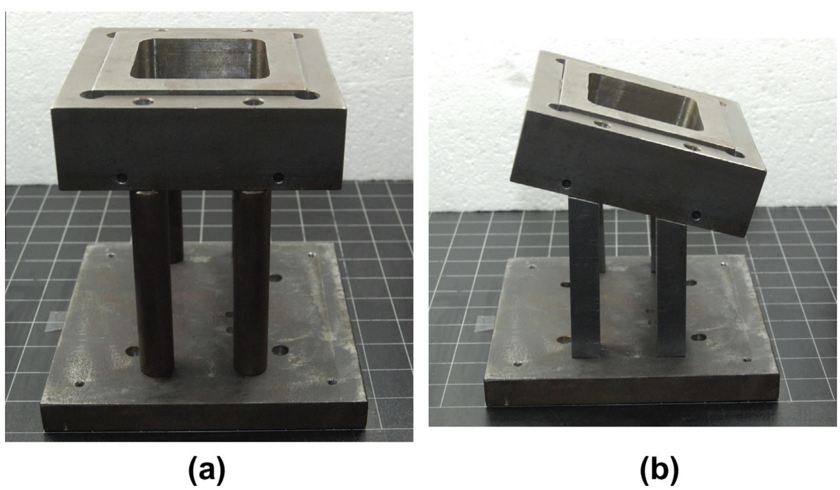


**Fig. 1.** Inclination angles devices employed to perform the oblique impact tests: (a) 0° and (b) 15°.

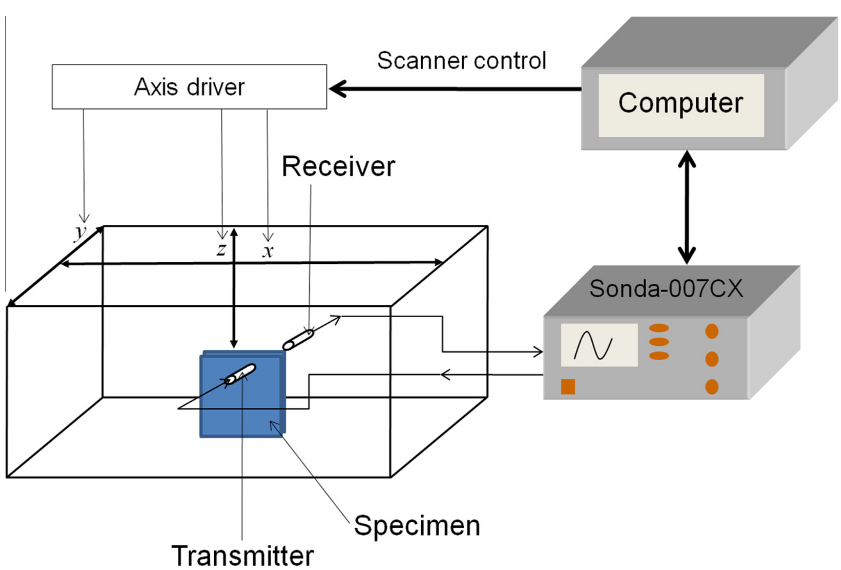


**Fig. 2.** Experimental set-up for C-scan inspection of impacted sandwich structures.

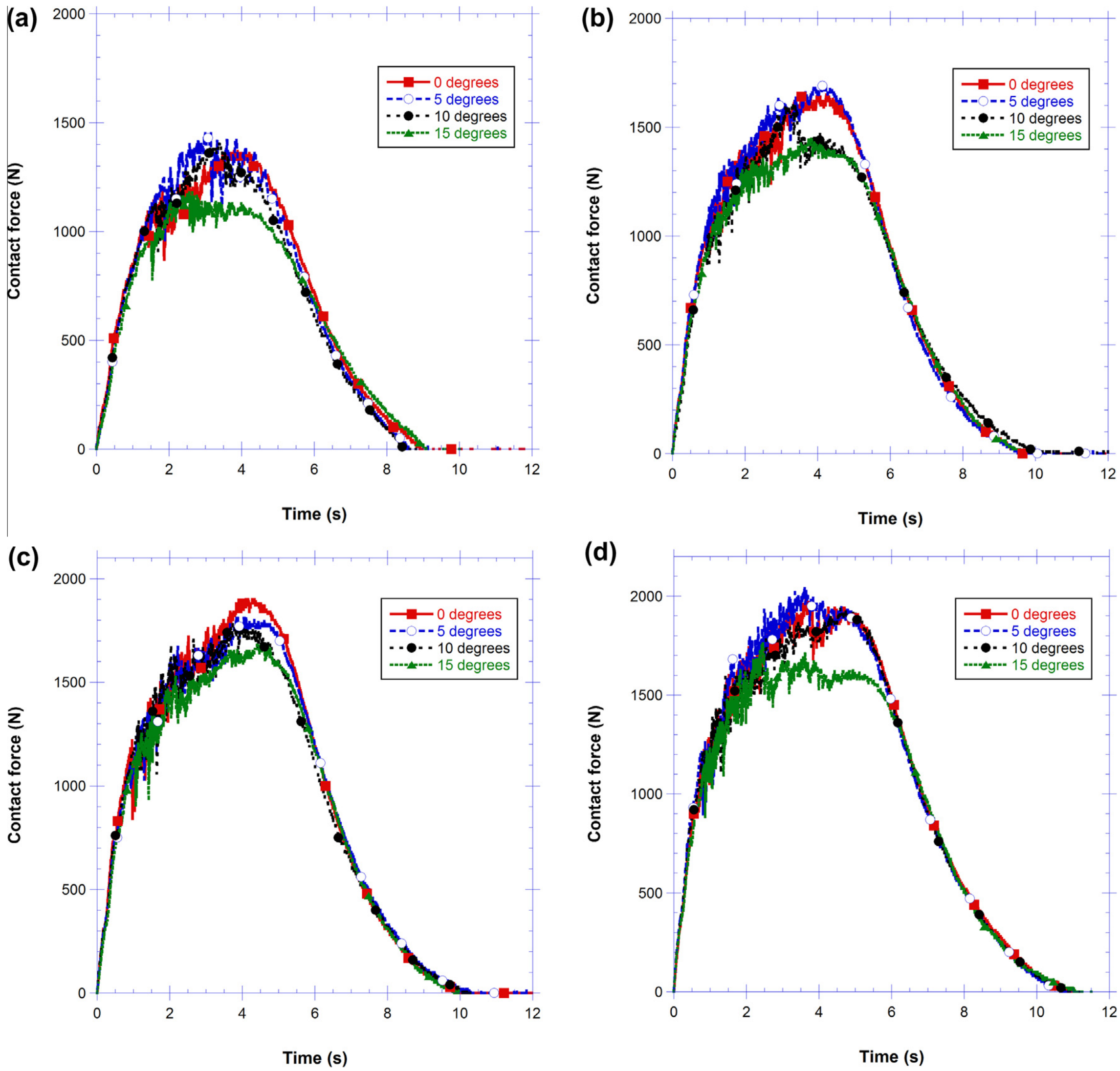


**Fig. 3.** Contact force vs. time curves at theoretical impact energy: (a) 3 J, (b) 5 J, (c) 7 J, (d) 10 J.

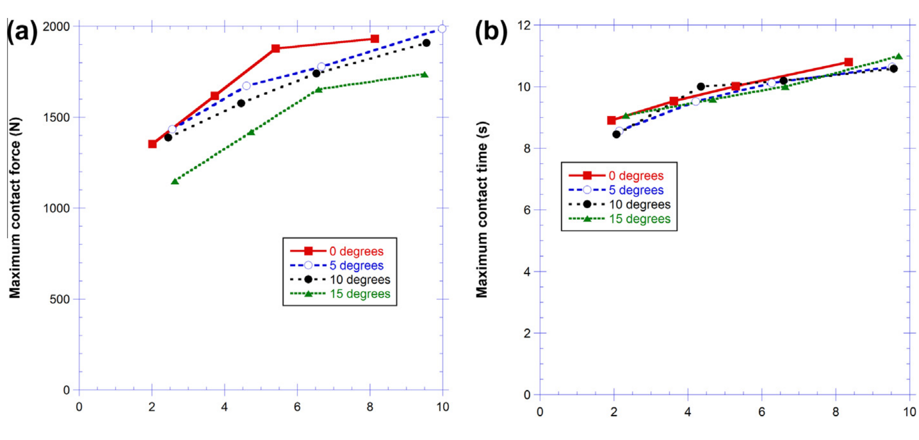


**Fig. 4.** Variations of main impact parameters with impact energy: (a) peak force, (b) maximum contact time.

An experimental device was designed to carry out oblique impact tests on sandwich structures. The device has enough stiff ness to ensure that the transmitted force during the impact does not affect the results. The device (Fig. 1) is assembled with the following pieces (especially manufactured for this work): a support for the device, a support to place the specimen, a cover for the specimen, and four columns. One of the extremes of the columns is flat and connected with bolts to the device support, while the

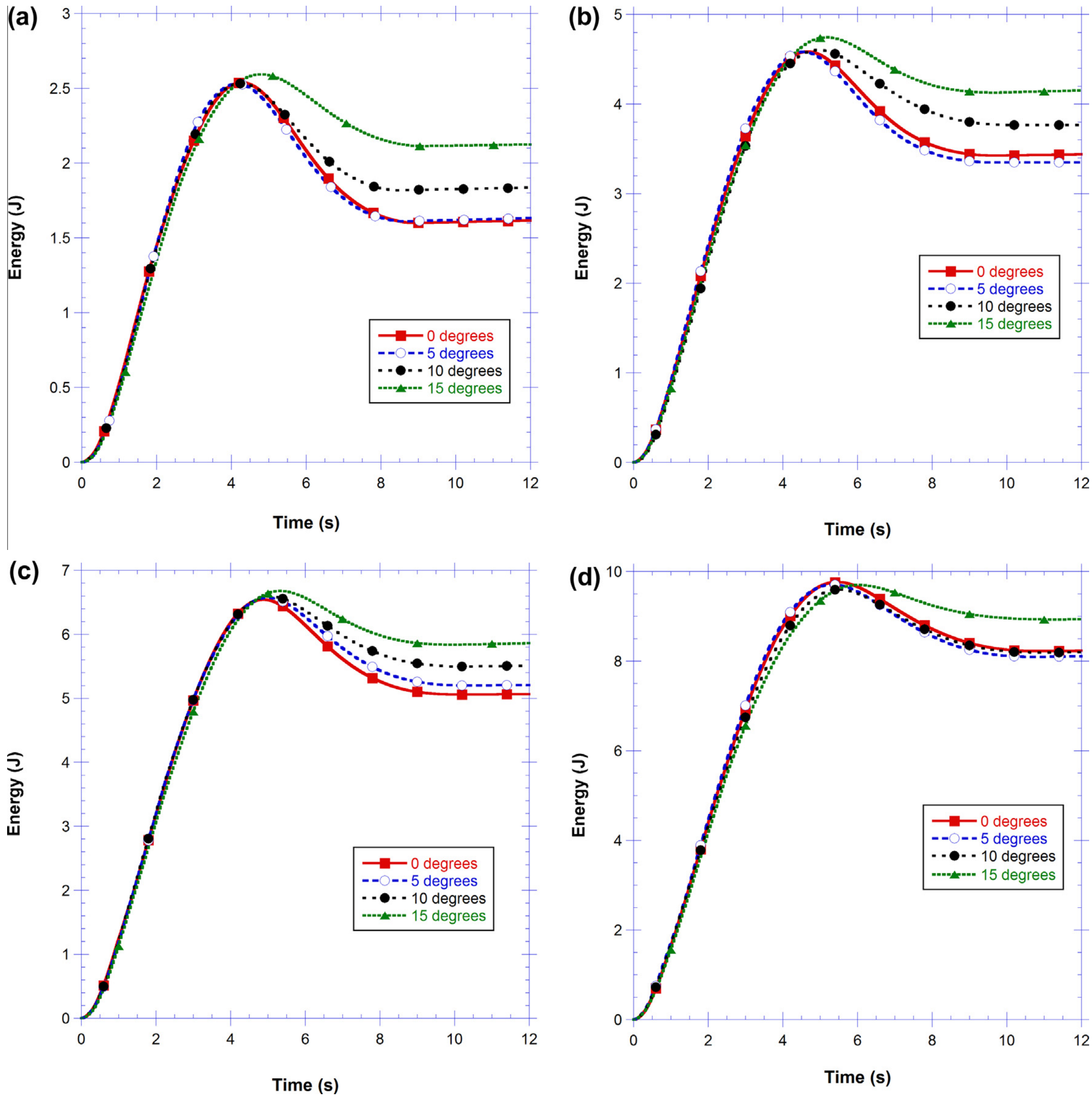


**Fig. 5.** Energy vs. time curves at theoretical impact energy: (a) 3 J, (b) 5 J, (c) 7 J, (d) 10 J.

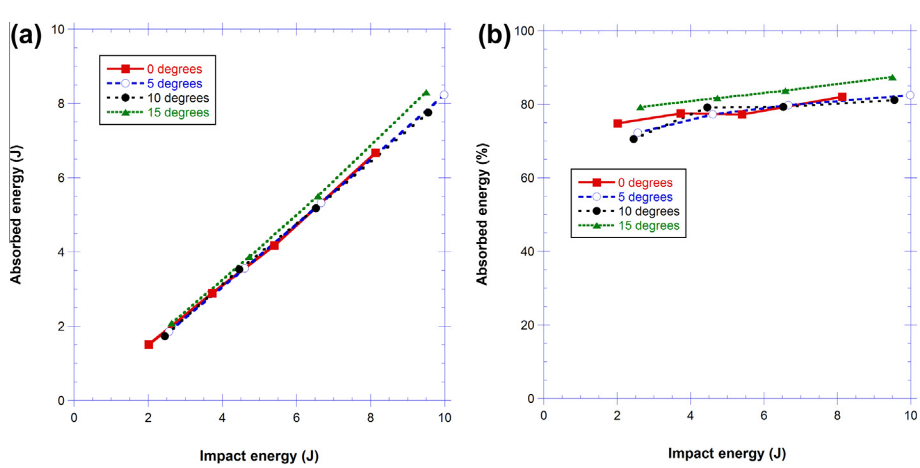


**Fig. 6.** Energy absorbed vs. impact energy: (a) absolute value, (b) percentage.

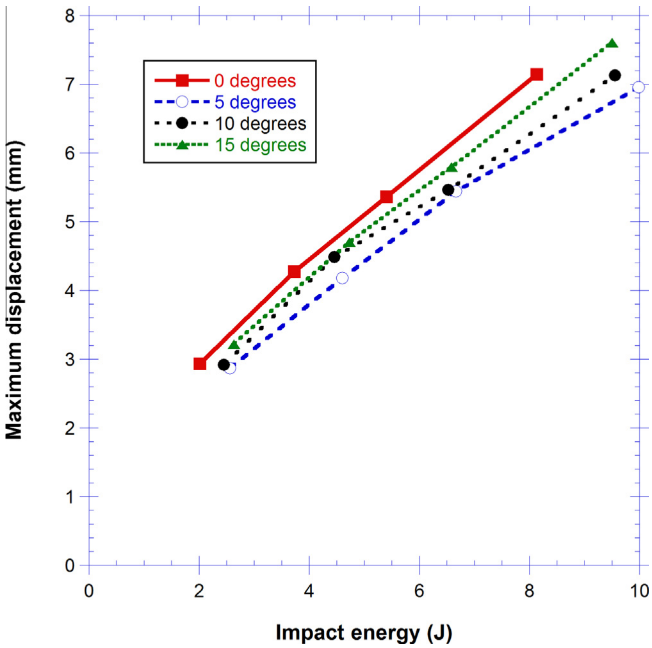


**Fig. 7.** Maximum impact displacement vs. impact energy.

other extreme has the selected inclination to conduct each of the tests, and is connected with bolts to the specimen support. Finally, as a consequence, four groups of columns were manufactured, one for each impact angle.

From each test, a record of the force applied by the impactor on the specimen was obtained. From this record, the displacement of the contact point and the absorbed energy can be determined by successive integrations [21].

All tests were recorded using a high speed video camera APX PHOTRON FASTCAM to obtain an accurate estimation of impact and rebound velocities. There may be a possible friction between the impactor set and the rails of the drop tower. This friction is not considered by the drop weight tower controller when the initial velocity of the impact event is given; therefore, there may be a possible error in the impact velocity measured by the height from which the impactor is dropped. Impact and rebound velocities were calculated evaluating the distance travelled by the impactor in several consecutive frames. The number of frames were selected according to a previous study to ensure an accurate estimation of the velocity [22]. From these velocities, the impact and absorbed energies were estimated.

After the impact tests, specimens were inspected both visually and by C Scan technique, to analyse the damage caused by the impact. A C Scan by air coupled non contact ultrasounds (ACU) was used to prevent the specimens from getting wet. This experimental equipment (Fig. 2) was manufactured by TECNITEST, and it is composed of the following components: a computer, the Sonda 007CX, two transducers (both of 225 kHz) where one (transmitter) sends out the ultrasonic pulse and the other (receiver) receives the signal, and finally an automatic system of movement for the inspections.

### 2.3. Experimental results

#### 2.3.1. Contact force and contact time

Contact force curves as a function of time for every tested angle, are presented in Fig. 3. All the traces show the same trend, and the load and unloading part of the curve are smooth; however, the

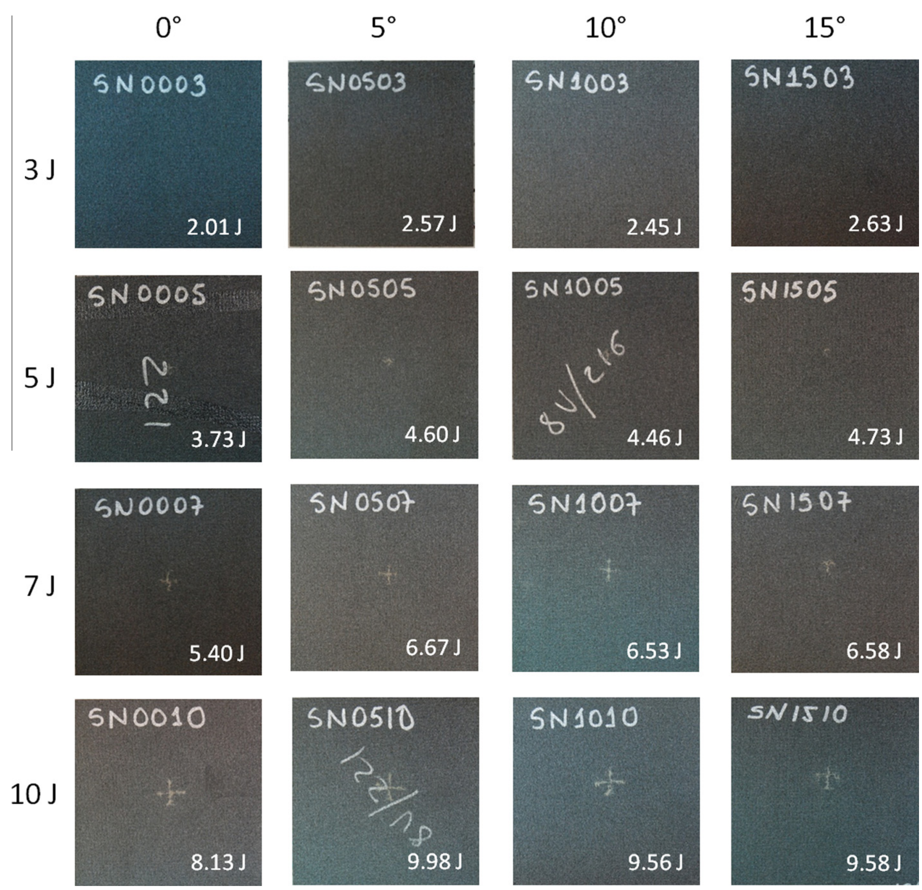


**Fig. 8.** External impact damage of composite sandwich plates for different oblique angles and impact energies.

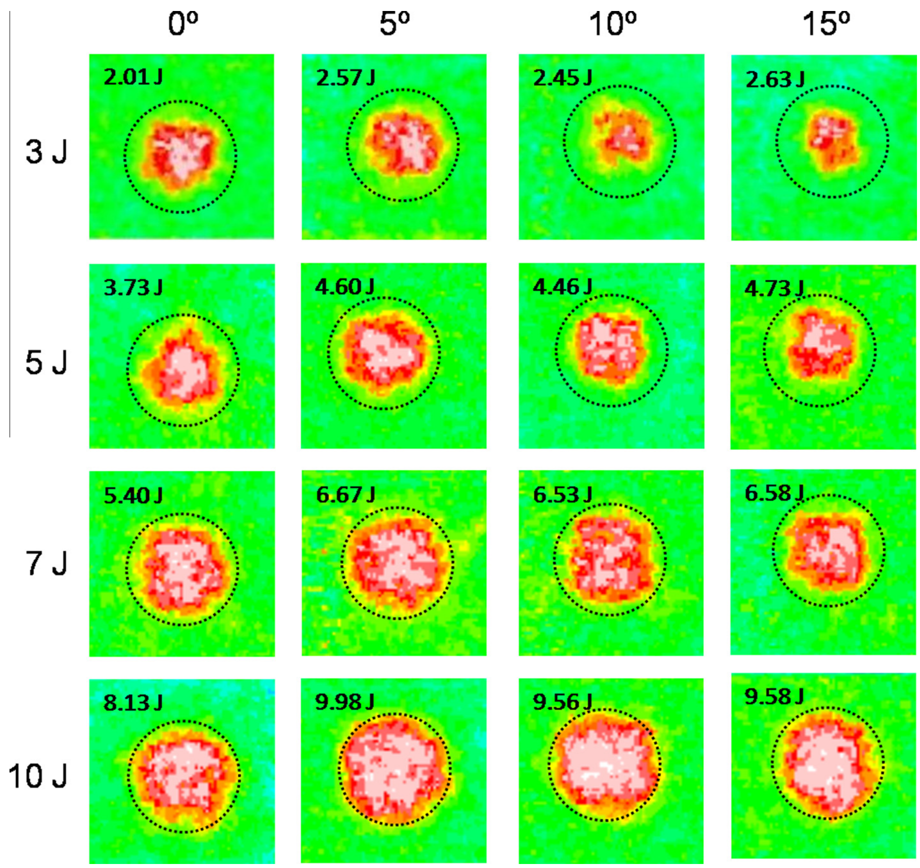


**Fig. 9.** C-scan images for different oblique angles and impact energies.

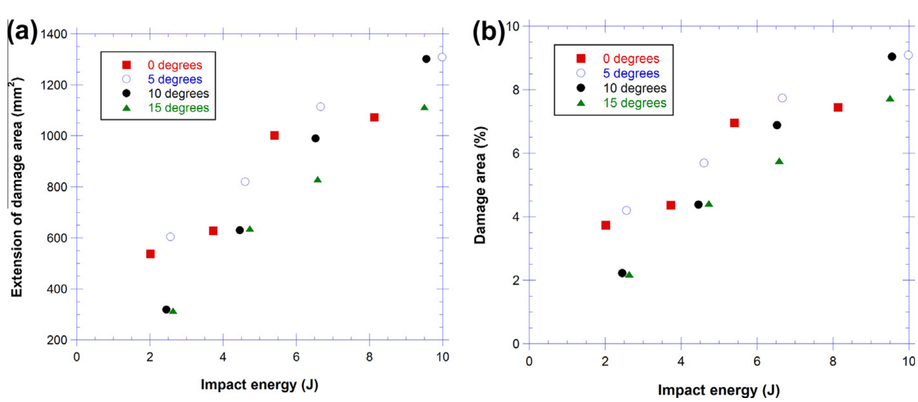


**Fig. 10.** Extension of damaged area vs. impact energy: (a) absolute value, (b) percentage.

drops and noise observed when the maximum contact force is reached, suggest damage in both the upper face sheet and honeycomb core, even at the lowest impact energy tested, in which no visible damage was found in the upper face sheet. The lower face sheet did not fail, or was visibly damaged, during the experimental tests.

The maximum contact force (peak load) clearly rise with increasing impact energy until a maximum is reached (Fig. 4(a)); on the contrary, the contact time slightly increase and remains almost constant (Fig. 4(b)). Contact force histories at 0° and 5° are almost coincident, and differences both in peak load and contact time are within the experimental scattering. At impact angle of 15°, differences are strongly visible in terms of peak force, which decreases with increasing impact angle. The maximum contact time slightly increase with increasing impact energy, but differences in terms of impact angle are negligible; this is more noticeable at higher impact energy levels, in which the unloading part of curves in Fig. 2 is almost coincident. As a result, the peak force decrease with increasing impact angle, but contact time is independent of this parameter.

### *2.3.2. Energy and maximum displacement*

Typical energy as a function of time curves, are shown in Fig. 5. In general, absorbed energy increases with increasing impact energy. The composite sandwich plates tested at the lowest impact energy have a moderate energy absorption level, typical of composite laminates. At this point, not visible damage in the upper face sheet of the sandwich structure was observed; whereas at higher impact energies, damage in the upper face sheet was completely visible, and the composite sandwich plates showed more impact energy absorption. Generally, results at 0° and 5° are almost coincident, and their differences are negligible; however, at impact angle of 10°, results in energy  time curves show some differences, and the energy absorbed is slightly higher than the observed at lower impact angles.

To confirm this observation, the absorbed energy as a function of impact energy for every impact angle, is presented in Fig. 6.

The energy absorption increase sharply with increasing angle (Fig. 6(a)), but differences in percentage are less strong than expected, and only impact angle of 15° results show some differences in energy absorption when compared to the other results (Fig. 6(b)). This coincides with the observations made in the previous section for the maximum contact force: between impact angles of 10  15° there is a change in the impact response of the composite sandwich plates. Results for 0°, 5° and 10° are almost coincident, while the energy absorption for 15° is slightly higher when compare to the other results; thus, absorbed energy increase with increasing impact angle.

Fig. 7 shows the variation of impactor maximum displacement with impact energy. The maximum displacement sharply increases with rising impact energy. Differences between different angles are within the scattering; as a result, maximum displacement is another independent parameter of impact angle.

*2.3.3. Damage evaluation*

External damage caused by the impact was observed visually on the upper face sheet (impacted face sheet). Fig. 8 shows the damage shape after low velocity impact at theoretical energies 3 J, 5 J, 7 J, and 10 J, for sandwich plates tested at 0°, 5°, 10°, and 15°. Measured impact energy is specified inside of each specimen image. No damage was observed visually in sandwich plates tested at 3 J. At impact energy of 5 J, the damage started with a quite small indentation. From this impact energy, the damaged area became cross shaped (typical damage shape in woven laminates under impact), increasing in the fibre direction with impact energy. At normal impact, the damage was cross shaped and perfectly symmetric, whereas at the largest impact angle tested, the vertical crack favoured the direction of the impact.

Additionally, the damaged area of specimens was estimated from the C Scan images. Fig. 9 shows the C scan images for the theoretical impact energies (3 J, 5 J, 7 J, and 10 J) and the different angles of obliquity. As in Fig. 8, measured impact energy is specified inside of each specimen C scan image. All images have a dotted circle with the same size to compare the damaged areas. The damage increases significantly with the impact velocity for all angles analysed. It is observed that the extension of the damaged area is similar at 0°, 5° and 10°, being smaller for 15°. For higher impact angles, the impactor specimen contact is smaller, being the damaged area minor, and more localised.

The C scan images allow measuring the damaged area using image processor software. In Fig. 10, the damage area as a function of the impact energy is represented for all impact angles studied. The damaged area increases with impact energy. No differences were observed between damaged areas at 0° and 5°. At 10° and low impact energies, damaged areas are found to be similar to the one obtained at 15°; however, at higher impact energies the area is comparable to those of 0° and 5°. For all impact energies analysed, damaged area is always the smallest at impact angle of 15°.

Usually, for composite sandwich structures, the damaged area increases with the impact energy, being therefore greater the absorbed energy. This behaviour is observed for all the impact angles analysed in this work. However, at impact angle of 15°, the damaged area is smaller compared to the other impact angles studied (Figs. 9 and 10) but the absorbed energy level is higher (Fig. 6).This can be due to the fact that the damaged area measured by C scan images, is a projection on a plane of the overall damage; not being identified the different damage mechanisms.

## 3. Numerical modelling

A finite element model is implemented to predict the contact force and behaviour of honeycomb sandwich plates under both normal and oblique impacts. First, the model is validated for impact angles analysed experimentally (0°, 5°, 10°, and 15°), and then impact angles difficult to perform experimentally (30°, 40°, and 50°) are studied.

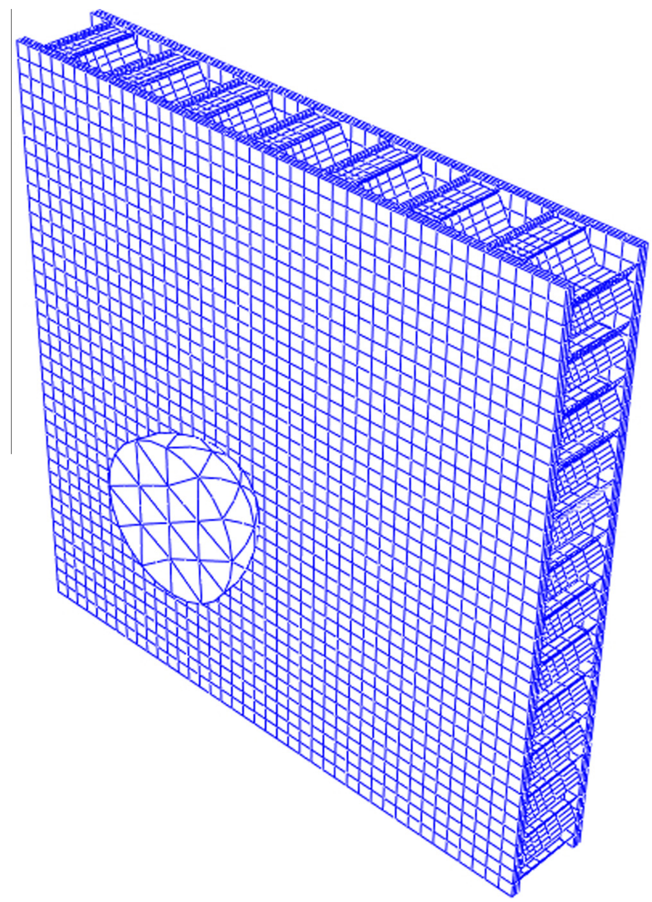

**Fig. 11.** Mesh of the model.

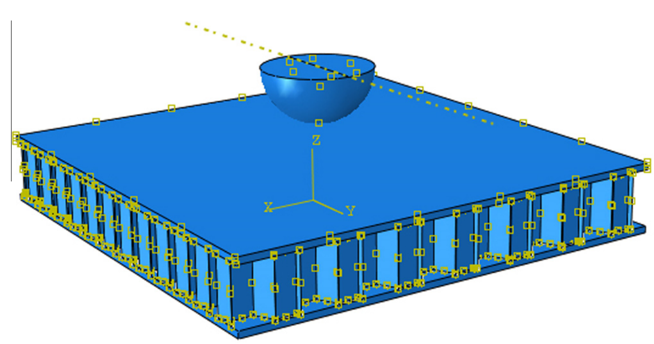


**Fig. 12.** Scheme of the impact numerical model (normal impact conditions).

### 3.1. Model description

The oblique impact model developed in this work reproduces the geometries of the specimens and the impact conditions tested experimentally. No quarter model is used because the obliquity of the problem does not allow symmetry. The model is implemented in Abaqus/Explicit and the meshing is carried out using 8 node continuum shell elements with reduced integration (SC8R) for the face sheets, 4 node shell elements with reduced integration (S4R) for the core, and a modified 10 node tetrahedral element (C3D10M) for the impactor (Fig. 11). The impactor is meshed using 138 elements, the core with 18,688 elements, and the face sheets with 9600 elements.

Fully clamped boundary conditions are applied to the external edges of the plate, and an initial velocity is imposed on the projectile in order to reproduce the experimental tests (Fig. 12). As no plastic deformation was observed experimentally in the projectile, a linear elastic behaviour is used for the steel impactor. The face sheets are modelled as linear elastic up to failure. A failure criterion and a procedure to degrade mechanical properties after failure are used to define the anisotropic mechanical behaviour of the composite face sheets. The model applied for damage initiation and evolution implemented in Abaqus/Explicit is based on the Hashin failure criteria for the initiation, and fracture energies for the damage evolution. Finally, the core is modelled with elastic perfectly plastic behaviour, where the properties needed are taken from the literature. The mechanical properties of the materials used are shown in Table 1.

### 3.2. Model validation

To validate the model with the results obtained experimentally, four different impact angles (0°, 5°, 10° and 15°) and four impact energies (3 J, 5 J, 7 J and 10 J) are analysed. The maximum contact force and time of the impact tests are the parameters selected to validate the model. In order to simplify the results, only the comparison between experimental and numerical contact force curves for 5° and 15° are shown (Fig. 13).

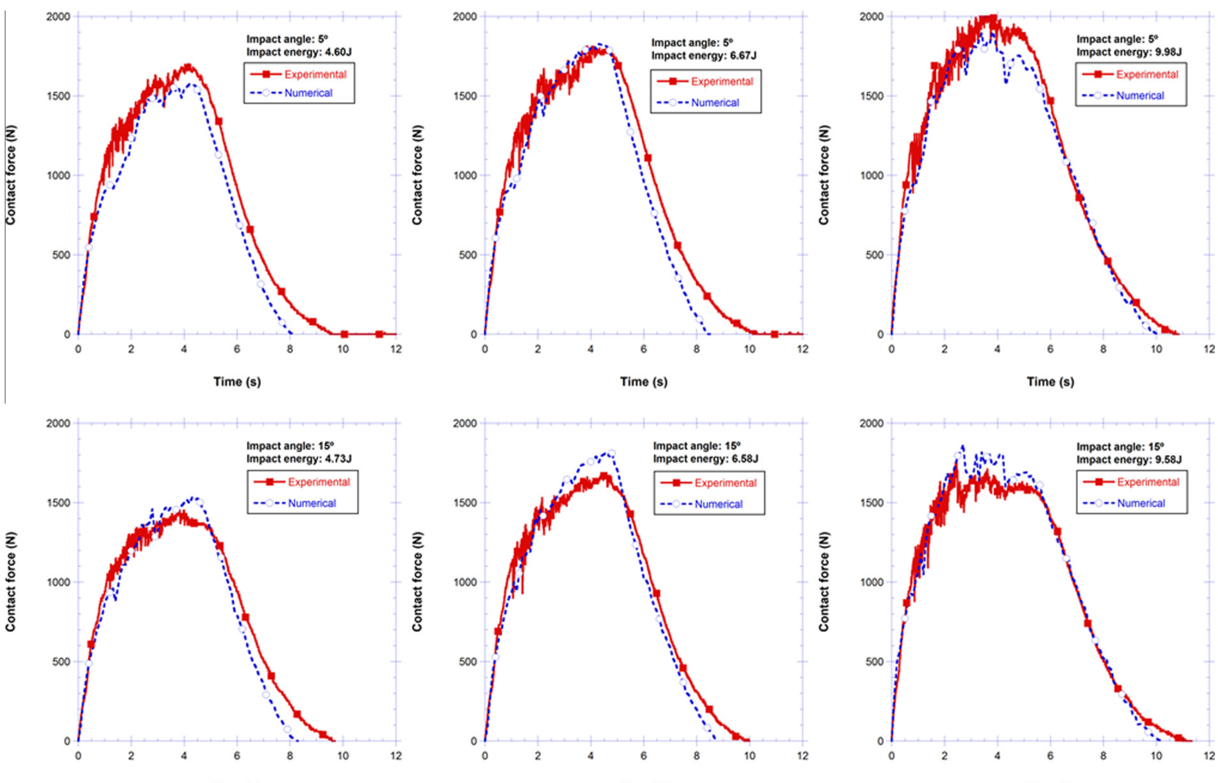


**Fig. 13.** Comparison between experimental and numerical contact force curves for 5° (top) and 15° (bottom) impact angles and for 5 J, 7 J and 10 J (from left to right) approximately impact energies.

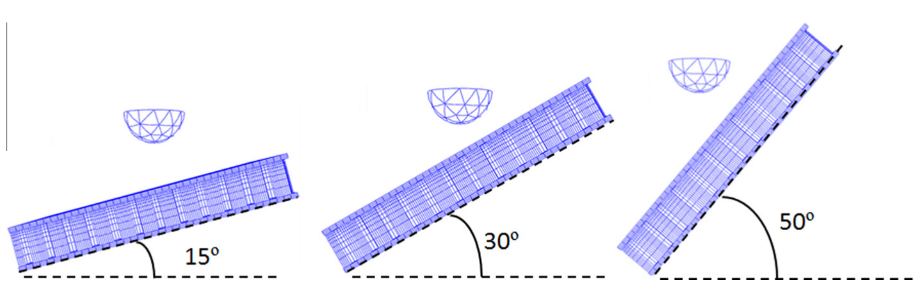


**Fig. 14.** Some impact angles analysed.

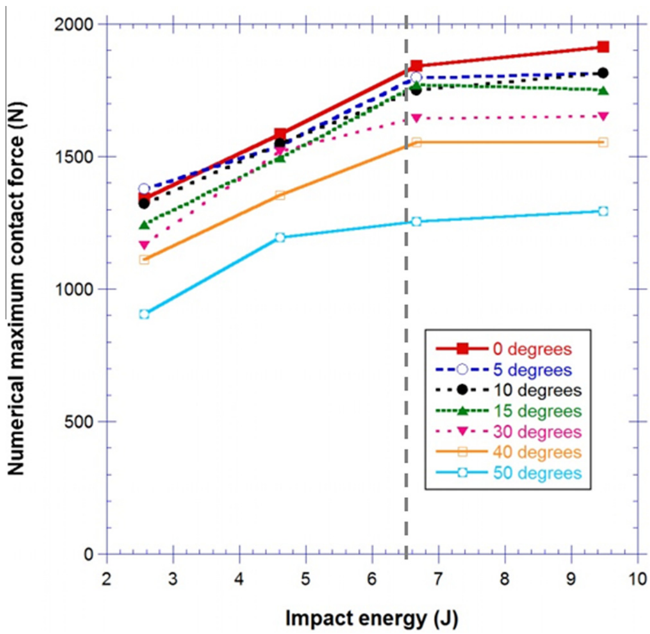


**Fig. 15.** Influence of impact angle on the maximum contact force vs. impact energy.

The difference between experimental and numerical contact force for all the impact angles and impact energies studied is so close, being the maximum difference of 8.59%. In terms of maximum contact time, differences between numerical and experimental results decrease as the impact energy increase, being the maximum difference of 16%.

Fig. 13 shows a good correlation between numerical and experimental contact force, the shape of the curves is nearly identical. Generally, the numerical model slightly overestimates the experimental results. This behaviour is observed in all the cases analysed.

Therefore, from Fig. 13 and from the rest of the results analysed for different impact angles and impact energies, the formulation of the numerical model enables an accurate estimation of the contact force, and can be validated.

### 3.3. Contact force analysis

Once the model is validated, impact angles difficult to perform experimentally, are analysed (30°, 40°, and 50°). The obliquity of the impact is given by rotating the plate the corresponding angle, as shown in Fig. 14. This angle corresponds to the angle between the axis of the impactor, and the normal to the plate.

Influence of impact angle on the maximum contact force as a function of the impact energy, is represented in Fig. 15. Smaller angles show similarities (contact forces results are very close), while over 15° differences are more visible. In addition, maximum contact force decreases while increasing impact angles. At low impact energy levels, below 6.5 J, the maximum contact force increases almost linearly with increasing impact energy.

For impact energies higher than 6.5 J, the maximum contact force remains almost constant. Additionally, at impact energy levels above 4.5 J, damage on the upper face sheet is observed, and the Nomex core starts crushing. As the typical stress strain curve for a honeycomb structure presents three different regions (linear, plateau, and densification [23]), the maximum contact force observed in the sandwich structure remains almost constant when the honeycomb core is crushed until the plateau stage, in which the strain increases whereas the load remains almost constant.

## 4. Conclusions

In this study the low velocity oblique impact response for composite sandwich structures has been studied experimentally under four impact energy levels and four different impact angles: 0°, 5°, 10° and 15°. The considered sandwich structure consisted of two composite carbon/epoxy face sheets, and a Nomex honeycomb core. The impact tests were performed to analyse the influence of the impact angle on the main impact parameters, and non destructive techniques were used to measure quantitatively the resulting damaged area of the core.

The damaged area was observed to decrease with increasing impact angle, as the contact area between impactor and upper face sheet decrease with the angle of obliquity. From the tests, it was observed that the maximum contact force (peak force) and absorbed energy decreased with increasing impact angle, whereas the contact time and maximum impactor deflection were independent on this parameter. Results for 0°, 5° and 10° impact angles were found similar, and differences were more noticeable at impact angle of 15°.

To analyse in detail the evolution of the maximum contact force, finite element models simulating oblique impact at 30°, 40°, and 50°, were developed using Abaqus/Explicit code. The maximum contact force increases with the impact energy until a certain value in which remains almost constant, suggesting that the core crushing process is important during the impact event. In addition, the maximum contact force decreases with increasing angle, as a result higher impact energy levels are needed to produce damage in both the upper face sheet and core.

## References


[1] Zonghong X, Vizzini AJ, Qingru T. On residual compressive strength prediction of composite sandwich panels after low-velocity impact damage. Acta Mech Solid Sin 2006;19(1):9–17.
[2] Davies GAO, Hitchings D, Besant T, Clarke A, Morgan C. Compression after impact strength of composite sandwich panels. Compos Struct 2004;63:1–9.
[3] Mines RAW, Worrall CM, Gibson AG. Low velocity perforation behavior of polymer composite sandwich panels. Int J Impact Eng 1998;21:855–79.
[4] Akil Hazizan MD, Cantwell WJ. The low velocity impact response of foam-based sandwich structures. Compos Part B 2002;33:193–204.
[5] Schubel PM, Luo J-J, Daniel IM. Low-velocity impact behaviour of composite sandwich panels. Compos Part A 2005;36(10):1389–96.
[6] Icardi U, Ferrero L. Impact analysis of sandwich composites based on a refined plate element with strain energy updating. Compos Struct 2009;89:35–51.
[7] Ivañez I, Santiuste C, Sanchez-Saez S. FEM analysis of dynamic flexural behaviour of composite sandwich beams with foam core. Compos Struct 2010;92:2285–91.
[8] Buitrago BL, Santiuste C, Sanchez-Saez S, Barbero E, Navarro C. Modelling of composite sandwich structures with honeycomb core subjected to high-velocity impact. Compos Struct 2010;92(9):2090–6.
[9] Ivañez I, Santiuste C, Barbero E, Sanchez-Saez S. Numerical modelling of foam-cored sandwich plates under high-velocity impact. Compos Struct 2011;93 (9):2392–9.
[10] Ivañez I, Sanchez-Saez S. Numerical modelling of the low-velocity impact response of composite sandwich beams with honeycomb core. Compos Struct 2013;106:716–23.
[11] Ivañez I, Barbero E, Sanchez-Saez S. Analytical study of the low-velocity impact response of composite sandwich beams. Compos Struct 2014;111:459–67.
[12] Sierakowski LR, Chaturvedi SK. Dynamic loading and characterization of fibre-reinforced composites. John Wiley & Sons; 1997.
[13] Wang T, Yu W, Dong S, Gao Y. Numerical simulation of penetration effect of the rhombic fragment on square honeycomb sandwich plate. Appl Mech Mater 2012;466–467:347–51.
[14] Navarro P, Aubry J, Marguet S, Ferrero J-F, Lemaire S, Rauch P. Experimental and numerical study of oblique impact on woven composite sandwich structure: influence of the firing axis orientation. Compos Struct 2012;94 (6):1967–72.
[15] Navarro P, Aubry J, Marguet S, Ferrero J-F, Lemaire S, Rauch P. Semi-continuous approach for the modeling of thin woven composite panels applied to oblique impacts on helicopter blades. Compos Part A: Appl Sci Manuf 2012;43 (6):871–9.
[16] Pascal F, Navarro P, Marguet S, Ferrero J-F, Aubry J, Lemaire S. Study of medium velocity impacts on the lower surface of helicopter blades. Proc Eng 2014;88 (C):93–100.

[17] Pascal F, Navarro P, Marguet S, Ferrero JF, Aubry J, Lemaire S. Experimental and numerical study of oblique impact on helicopter blades – influence of the curvature. In: 16th European conference on composite materials (ECCM 2014), Seville; 22–26 June 2014.

[18] Navarro P, Pascal F, Aubry J, Marguet S, Ferrero JF, Lemaire S, et al. Semi-continuous approach for the study of impacts on woven composite laminates: modeling interlaminar behavior with a specific interface element. Int J Impact Eng 2015;75:184–93.

[19] Zhou J, Hassan MZ, Guan Z, Cantwell WJ. The low-velocity impact response of foam-based sandwich panels. Compos Sci Technol 2012;72:1781–90.

[20] Sheikh Md, Fadzullah SH, Cantwell WJ. The effect of angle of incidence on the impact response of composites and sandwich structures. In: 15th European conference on composite materials (ECCM15), Venice; 24–28 June 2012.

[21] Sanchez-Saez S, Barbero E, Navarro C. Compressive residual strength at low temperatures of composite laminates subjected to low-velocity impacts. Compos Struct 2008;85:226–32.

[22] García-Castillo SK, Buitrago BL, Barbero E. Behavior of sandwich structures and spaced plates subjected to high-velocity impacts. Acta Mech Solid Sin 2011;32 (2):290–6.

[23] Gibson LJ, Ashby MF. Cellular solids: structure and properties. Cambridge University Press; 1997.